International Journal of Scientific Research & Engineering Technology (IJSET)
ISSN: 2356-5608, Vol.3, issue 2

Charge Transfer and Transport Properties in P3HT and P3HT:Graphene Based Organic Solar Cells

Rabeb Bkakri[#1] , Nadia Chehata[#2], , Olga Evgenievna Kusmartseva[*3], Feodor Kusmartsev[*4], Mo Song[♦5], Abdelaziz Bouazizi[#6]

[#]*Laboratoire de la Matière Condensée et des Nanosciences*
Faculté des Sciences de Monastir, Avenue de l'environnement, 5019 Monastir, Tunisie
[1]bkakrirabeb@hotmail.com
[2]nadiachehata2@gmail.com
[6]abdelaziz.bouazizi@yahoo.fr

[*]*Physics Department, Loughborough University, Leicestershire, LE11 3TU, United Kingdom*
[3]O.E.Kusmartseva@lboro.ac.uk
[4]f.kusmartsev@lboro.ac.uk

[♦]*Materials Department, Loughborough University, Leicestershire, LE11 3TU, United Kingdom*
[5]m.song@lboro.ac.uk

***Abstract*—We have investigated the effects of the incorporation of graphene in the matrix of regioregular poly (3-hexylthiophene-2, 5-diyl) (RR-P3HT) on the charge transfer and transport processes. The addition of graphene to P3HT reduces the RMS roughness of the thin film. The presence of the G-band of graphene in the Raman spectrum of *P3HT:Graphene* nanocomposite proves that the graphene are well inserted in the P3HT matrix. The charge transfer at the interfaces between P3HT and graphene and the charge transport processes are studied through photoluminescence and current density-voltage (J-V) measurements.**

***Keywords*—polymers; thin films; charge transfer; charge transport; photovoltaic**

I. INTRODUCTION

Graphene is a flat monolayer of sp^2 hybridized carbon atoms stacked into a two-dimensional (2D) honeycomb lattice which is recognized as one of the strongest materials in the world due to its excellent properties including high electrical conductivity (10^8 $S.m^{-1}$) and thermal conductivity (~5000 W. $m^{-1}.K^{-1}$), high electron mobility at room temperature (250.000 $cm^2.Vs$), high transparency (absorbance of 2.3 %), and large specific surface area (2.63×106 $m^2.Kg^{-1}$). It was also demonstrated that this material is stable at ambient conditions [1, 2, 3, 4]. It is a basic structure for the building of graphitic materials of all other dimensionalities. It can be wrapped into 0D fullerenes, rolled into 1D carbon nanotubes or stacked into 3D graphite. Organic nanocomposites based on polymer and graphene have shown potential interest in the field of optoelectronic and especially for photovoltaic application. Several efforts have been made in last few years to improve the efficiencies of *Polymer:Graphene* photovoltaic devices [5, 6, 7, 8, 9]. The main problem in the elaboration of *Polymer:Graphene* nanocomposites is the dispersion of the graphene layers in the polymer matrix. Therefore, it's important to select the suitable proportion of graphene to avoid the agglomeration of the graphene layers. To further improve the power conversion efficiency of the photovoltaic cells, it is important to use high-mobility polymers as donor of electrons material. In this work we have used expandable graphite oxide (EGO) for the elaboration of the graphene layers. EGO could be dispersed in organic solvent without any assistance of chemical treatment. The attached oxidants groups in the graphene layers prevent the agglomeration of the graphene layers. We have incorporated the graphene layers in the RR-P3HT matrix to elaborate bulk-heterojunction solar cell, since P3HT is known by the high mobility of holes (0.2 $cm^2.V^{-1}.\ s^{-1}$) compared to other conjugated polymer [10]. P3HT and graphene act as electron-donating and electron-accepting materials, respectively. In this study we present a comparison between the performances of the ITO/P3HT/Au and ITO / P3HT:Graphene /Au solar cells.

II. EXPERIMENTAL PROCEDURE

A. Materials

RR-P3HT (RR = 96.3 %) with a molecular weight M_w = 77.5 $g.mol^{-1}$ is provided by Ossila Ltd Kroto Innovation Centre. The graphene oxide layers are prepared by the dissolution of EGO in DMF. EGO was obtained by the oxidation of expandable graphite (EG) following Hummer's

method [11]. The oxidation of EG was provided by Chinese Qing Dao Graphite Company.

B. *Devices elaboration*

The P3HT was dissolved in chloroform at a concentration of 5 mg/ml. Expandable graphite oxide was dispersed in N, N-dimethylformamide (DMF) with a composition of 1.5 wt.% and subjected to strong ultrasonic treatment (Fisher Scientific Sonic Dismembrator Model 500, 300 W) for 1 hour at room temperature. The obtained solutions are mixed and stirred for 15 min at a temperature of 50 ° C, and then sonicated for 1 hour at room temperature. The solutions of P3HT and *P3HT:Graphene* nanocomposite were spin coated onto ITO-coated glass substrates and then annealed under vacuum at T = 170°C for 10 min to remove the residual solvent. Back-contacts of Au were thermally evaporated on the top of the active layers, at a pressure of 10^{-6} Torr.

C. *Instrumentation*

Imaging of the surface of the thin films of P3HT and *P3HT:Graphene* nanocomposite, was carried out using an Atomic Force Microscope (Digital Instrument Vecco, Nanoscope, Dimension ^{TM} 3100) in the tapping mode. Raman and photoluminescence spectra were recorded using a Horiba Jobin Yvon HR Lab RAM Micro-Raman system with a laser line at 488 nm originating from an Ar^{+} laser. A 50 x objective lens was used to focus on the laser beam (about 1 µm spot size) and to collect the Raman signal in the backscattering configuration and an accurate calibration was carried out by checking the Si band at 520.7 cm^{-1}. All the spectra were recorded with a 600 lines/mm grating at the temperature T = 300 K under the same experimental conditions. The current-voltage characteristics were measured under illumination at room temperature with "Keithley 6430" source and a PC card for acquisition, using 100 W halogen lamp.

III. Results and Discussion

A. *Morphological Properties*

The AFM images of the thin films of P3HT and *P3HT:Graphene* nanocomposite deposited on ITO substrates are shown in Fig. 1. The surface of P3HT thin film shows bright areas corresponding to the P3HT nanowires. The P3HT nanowires are connected to each other forming large domains. However the AFM images of *P3HT:Graphene* nanocomposite show smaller bright area compared with the thin film of pristine P3HT. The observed changes in the surface of the thin film of *P3HT:Graphene* nanocomposite proves that the nanowires of P3HT are separated from each other after addition of the graphene layers. The RMS roughness of P3HT thin film is about 15.01 nm. After addition of 1.5 wt. % of graphene the RMS roughness decreases to 9.91 nm. The reduction of the RMS roughness after addition of graphene proves that the insertion of the graphene layers in the P3HT matrix serve to planarize the surface of the film.

Fig. 1 Example AFM height images of the thin films of P3HT (a), and

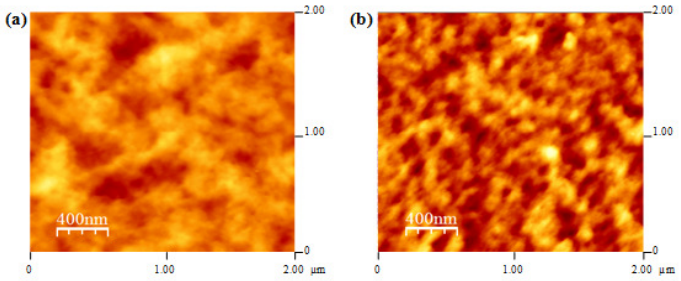

P3HT:Graphene nanocomposite (b).

B. *Raman and Photoluminescence measurements*

Raman spectroscopy is used in this work to confirm the presence of graphene in the P3HT matrix. The Raman spectra of the thin films of P3HT and *P3HT:Graphene* nanocomposite, shown in Fig. 2, are obtained under resonant excitation (488 nm). The Raman spctrum of P3HT thin film shows two vibrational modes associated with the conjugated backbone (π- electron delocalization) of P3HT: the C=C symmetric stretch mode at ~1445 cm^{-1} and the C-C stretch mode at ~1381 cm^{-1} within the thiophene rings. The two Raman modes of P3HT represent the origin of the electrical conductivity in conjugated polymer.

The Raman spectrum of graphene includes the following characteristics bands: the D band ~1340-1360 cm^{-1} is the representation of the disorder in the sp^2 hybridization [12], the G band ~1575-1604 cm^{-1}, and the 2D band ~ 2650-2695 cm^{-1} [13, 14, 15, 16]. This mode could be active if the ring is adjacent to a graphene edge or a defect [17, 18]. The position and the intensity of the G and 2D bands are related to the crystallinity, number of layers, and the type of substrate used to synthesize the graphene layers [19, 20]. Fig. 2(b) shows the Raman spectrum of the thin film of *P3HT:Graphene* nanocomposite. The Raman spectrum shows the feature peaks of P3HT and graphene. The presence of the two main Raman modes of P3HT, at ~1445 cm^{-1} and ~1381 cm^{-1}, proves that the P3HT nanowires remain unaltered after addition of graphene. We also observe the characteristic G-mode of graphene. The G-band of graphene results from the first order scattering of the E_{2g} in-plane vibrational modes [21, 22, 23]. The absence of the D band proves that we have a well ordered graphene [24]. The absence of the 2D band is due to the P3HT doping effect. In fact the theory predicts the intensity of the 2D Raman mode should decrease as electron-electron collisions increase strongly at high doping levels [25, 26].

International Journal of Scientific Research & Engineering Technology (IJSET)
ISSN: 2356-5608, Vol.3, issue 2
Copyright IPCO-2015-pp.89-94

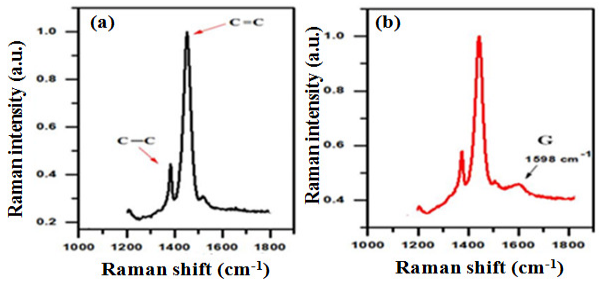

Fig. 1 Raman spectra of the thin films of P3HT (a), and *P3HT:Graphene* nanocomposite (b).

We have investigated the charge transfer process at the interface between P3HT and graphene using the photoluminescence spectroscopy. The PL spectra of P3HT and *P3HT:Graphene* nanocomposite shown in Fig. 3 are obtained using 488 nm excitation which lies within the absorption band of P3HT [27]. The PL spectrum of P3HT shows two strong peaks at 650 and 688 nm. These peaks are significantly quenched after addition of graphene. PL quenching in D:A blends upon photoexcitation of the donor is mostly due to energy or charge transfer at the interface between the donor and the acceptor of electrons as shown in different studies [28, 29, 30, 31]. There is no overlap between the emission spectrum of P3HT, which is situated between 600 and 750 nm as shown in Fig. 3, and the electronic absorption spectrum of graphene localized between 200 and 400 nm [32], which proves that the quenching of the PL intensity of P3HT with progressive addition of graphene is due to electrons transfer rather than resonance energy transfer process. Then the quenching of the PL intensity of P3HT is due to electrons transfer from P3HT to graphene rather than resonance energy transfer. The energy band diagram of P3HT and graphene is shown in Fig. 4. The graphene conduction and valence bands cross at the Dirac point, which defines the work function (W_f = 4.6 eV) [33]. The Fermi level (E_f) of graphene is situated below the LUMO level of P3HT which make the electrons transfer from P3HT to graphene energetically possible.

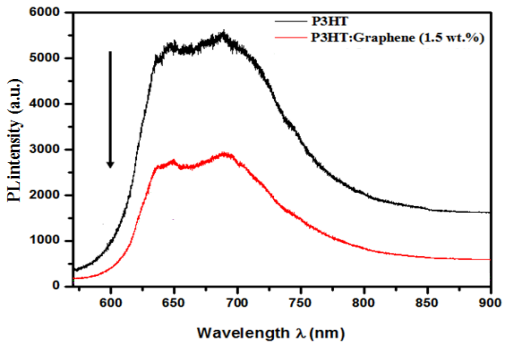

Fig. 3 Photoluminescence spectra of the thin films of P3HT (a), and *P3HT:Graphene* nanocomposite (b).

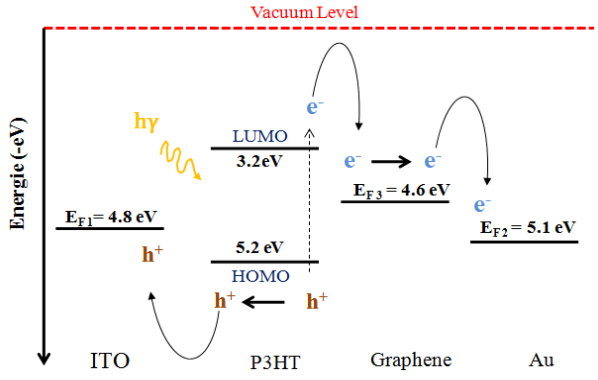

Fig. 4 Energy band diagram of the ITO/*P3HT:Graphene*/Au device.

C. Current Density–Voltage Characteristics

Fig. 5 shows the J-V characteristics of the ITO/P3HT/Au and ITO/*P3HT:Graphene*/Au photovoltaic devices under illumination. The current density J_{sc} and the open circuit voltage V_{oc} are extracted from the J–V curves. The fill factor (FF) defined as the ratio between the maximum power delivered to an external circuit and the potential power was calculated using the following expression [34]:

$$FF = \frac{Pmax}{Voc\ \ Jsc} = \frac{Vmax\ Jmax}{Voc\ Jsc} \qquad (1)$$

Where V_{max} and J_{max} are the open circuit voltage and the current density at the maximum power point of the J-V curve in the fourth quadrant, where the device operates as an electrical power source. The V_{oc} increase from 0.35 to 0.55 eV, and the J_{sc} increase from 4.25 x 10^{-4} to 9.93 x 10^{-4} for P3HT and *P3HT:Graphene* based devices, respectively. Then the fill factor increase from 29 to 41 % after addition of 1.5 wt.% of graphene to P3HT. The photovoltaic parameters of ITO/P3HT:Graphene/Au devices are enhanced compared with ITO/P3HT/Au device. The photovoltaic performances of the device are enhanced after addition of graphene due to the formation of continuous electrons pathways arising after an appropriate addition of graphene. In addition the formation of P3HT/Graphene interfaces improves the dissociation of the photogenerated excitons and the charge transfer processes as shown in the energy band diagram of ITO/P3HT:Graphene/Au structure in Fig. 4. The improvement of the photovoltaic performances of the device after addition of graphene is also attributed to the increase of the optical absorption properties of the device which increase the number of the photogenerated excitons. In addition the graphene layers are well dispersed in the P3HT matrix, as shown in the AFM images, which improve the charge transport properties of the device.

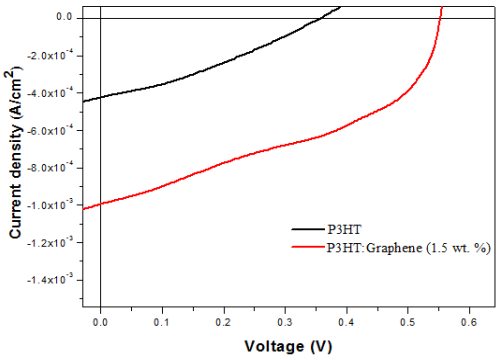

Fig. 5 J-V characteristics of the ITO/P3HT/Au, and ITO/*P3HT:Graphene* /Au solar cells.

IV. Conclusions

In this work we have studied the effect of the insertion of graphene in the P3HT matrix on the photovoltaic performances of the device. The AFM images of P3HT and *P3HT:Graphene* nanocomposites proves that the insertion of the graphene layers in the P3HT matrix serve to planarize the surface of the thin film. The presence of the G-band of graphene in the Raman spectrum of *P3HT:Graphene* nanocomposite confirm the presence of graphene in the P3HT matrix. The electrical measurements show that the photoconversion efficiency of the solar cell was significantly improved with the insertion of graphene in the P3HT matrix.

References

[1] K. S. Novoselov , A. K. Geim , S. V. Morozov , D. Jiang , Y. Zhang , S. V. Dubonos , I. V. Grigorieva , and A. A. Firsov, "Electric field effect in atomically thin carbon films, "*Science*, vol. 306, pp. 666–669, 2004.

[2] A. K. Geim, and K. S. Novoselov, "The rise of graphene," *Nat. Mater.,* Vol. 6, pp. 183–191, 2007.

[3] K. S. Novoselov, A. K. Geim, S. V. Morozov, D. Jiang, M. I. Katsnelson, I. V. Grigorieva, S. V. Dubonos, and A. A. Firsov, "Two-dimensional gas of massless Dirac fermions in Graphene," *Nature,* vol. 438, pp. 197–200, 2005..

[4] Y. Wang, D. Kurunthu, G. W. Scott, and C. J. Bardeen "Fluorescence quenching in conjugated polymers blended with reduced graphitic oxide," *J. Phys. Chem. C*, vol. 114, pp. 4153–4159, 2010.

[5] J. Liang, Y. Huang, L. Zhang, Y. Wang, Y. Ma, T. Guo, and Y. Chen, "Molecular-Level Dispersion of Graphene into Poly(vinyl alcohol) and Effective Reinforcement of their Nanocomposites ," *Adv. Funct. Mater.*, vol. 19, pp. 2297–2302, 2009.

[6] T. Ramanathan, S. Stankovich, D. A. Dikin, H. Liu, H. Shen, S.T. Nguyen, and L. C. Brinson, "Graphitic nanofillers in PMMA nanocomposites—An investigation of particle size and dispersion and their influence on nanocomposite properties," *J. Polym. Sci., Part B: Polym. Phys.*, vol. 45, pp. 2097–2112, 2007.

[7] X. Zhao, Q. Zhang, and D. Chen, "Enhanced mechanical properties of graphene-based poly(vinyl alcohol) composites," *Macromolecules*, vol. 43, pp. 2357–2363, 2010.

[8] J. Liang, Y. Xu, Y. Huang, L. Zhang, Y. Wang, Y. Ma, F. Li, T. Guo, and Y. Chen, "Infrared-triggered actuators from graphene-based nanocomposites," *J. Phys. Chem. C*, vol. 113, pp. 9921–9927, 2009.

[9] G. Eda, and M. Chhowalla, "Graphene-based composite thin films for electronics", *Nano Lett.,* vol. 9, pp.814 –818, 2009.

[10] M. Al-Ibrahim, H. Roth, U. Zhokhavets, G. Gobsch, and S. Sensfuss, "Flexible large area polymer solar cells based on poly(3-hexylthiophene)/fullerene," *Sol. Energy Mater. Sol. Cells*, vol. 85, pp. 13–20, 2005.

[11] P. Liu, K. Gong, P. Xiao, and M. Xiao, "Preparation and characterization of poly(vinyl acetate)-intercalated graphite oxide nanocomposite," *J. Mater. Chem.*, vol. 10, pp. 933– 935, 2000.

[12] M. S. Dresselhaus, A. Jorio, M. Hofmann, G. Dresselhaus, and R. Saito, "Perspectives on carbon nanotubes and graphene raman spectroscopy," *Nano. Lett.*, vol. 10, pp. 751–758, 2010.

[13] A. C. Ferrari, J. C. Meyer, V. Scardaci, C. Casiraghi, M. Lazzeri, F. Mauri, S. Piscanec, D. Jiang, K. S. Novoselov, S. Roth, and A. K. Geim, "Raman spectrum of graphene and graphene layers,", *Phys. Rev. Lett.*, vol. 97, 187401, 2006.

[14] A. C. Ferrari, "Raman spectroscopy of graphene and graphite: Disorder, electron–phonon coupling, doping and nonadiabatic effects," *Solid State Commun.*, vol. 143, pp. 47–57, 2007.

[15] A. Chunder, J. Liu, and L. Zhai, "Reduced graphene oxide/poly-(3-hexylthiophene) supramolecular composites," *Macromol. Rapid Commun.*, vol. 31, pp. 380–384, 2010.

[16] A. C. Ferrari, J. C. Meyer, V. Scardaci, C. Casiraghi, M. Lazzeri, F. Mauri, S. Piscanec, D. Jiang, K. S. Novoselov, S. Roth, and A. K. Geim, "Raman spectrum of graphene and graphene layers,", *Phys. Rev. Lett.*, vol. 97, 187401, 2006.

[17] A. Gupta, G. Chen, P. Joshi, S. Tadigadapa, and P. C. Eklund, "Raman scattering from high-frequency phonons in supported n-graphene layer films," *Nano. Lett.,* vol. 6, pp. 2667–2673, 2006.

[18] A. C. Ferrari, "Raman spectroscopy of graphene and graphite: Disorder, electron–phonon coupling, doping and nonadiabatic effects," *Solid State Commun.*, vol. 143, pp. 47–57, 2007.

[19] D. Graf, F. Molitor, K. Ensslin, C. Stampfer, A. Jungen, C. Hierold, and L. Wirtz, Raman imaging of graphene," *Solid State Commun.*, vol. 143, pp. 44–46, 2007.

[20] Y. Zhu , S. Murali , W. Cai , X. Li , J. W. Suk , J. R. Potts, and R. S. Ruoff, "Graphene and graphene oxide: synthesis, properties, and Applications," *Adv. Mater.*, vol. 22, pp. 3906–3924, 2010.

[21] A. C. Ferrari, J. C. Meyer, V. Scardaci, C. Casiraghi, M. Lazzeri, F. Mauri, S. Piscanec, D. Jiang, K. S. Novoselov, S. Roth, and A. K. Geim, "Raman spectrum of graphene and graphene layers,", *Phys. Rev. Lett.*, vol. 97, 187401, 2006.

[22] Z.H. Ni, W. Chen, X. F. Fan, J. L. Kuo, T. Yu, A. T. S. Wee, Z. X. Shen, "Raman spectroscopy of epitaxial graphene on a SiC substrate," *Phys. Rev. B*, vol. 77, pp. 115416, 2008.

[23] Y. Zhu , S. Murali , W. Cai , X. Li , J. W. Suk , J. R. Potts, and R. S. Ruoff, "Graphene and graphene oxide: synthesis, properties, and Applications," *Adv. Mater.*, vol. 22, pp. 3906–3924, 2010.

[24] D. M. Basko, S. Piscanec, and A. C. Ferrari, "Electron-electron interactions and doping dependence of the two-phonon Raman intensity in graphene," *Phys. Rev. B*, vol. 80, pp. 165413, 2009.

[25] D. M. Basko, S. Piscanec, and A. C. Ferrari, "Electron-electron interactions and doping dependence of the two-phonon Raman intensity in graphene," *Phys. Rev. B*, vol. 80, pp. 165413, 2009.

[26] N. Jung, N. Kim, S. Jockusch, N. J. Turro, P. Kim, and L. Brus, "Charge transfer chemical doping of few layer graphenes: charge distribution and band gap formation" *Nano Lett.,* vol. 9, pp. 4133–4137, 2009.

[27] V. Shrotriya, J. Ouyang, R. J. Tseng, G. Li, and Y. Yang, "Absorption spectra modification in poly(3-hexylthiophene):methanofullerene blend thin films," *Chem. Phys. Lett.*, vol. 411, pp. 138–143, 2005.

[28] R. Bkakri, A. Ltaief , N. Chehata, N. Chaaben, F. Saidi, and A. Bouazizi, "Charge transfer properties in PVK:PcH_2:C343:C_{60}/p-Si hybrid nanocomposites for photovoltaics," *Vacuum*, vol. 104, pp. 33–40, 2014.

[29] N. Chehata, A. Ltaief, A. Bouazizi, and V.T. Binth, "Charge transfer properties in poly(2-methoxy-5-(2-ethyhexyl-oxy)-*p*-phenylenevinylene) / carbon nanopearls nanocomposites," *J. Surf. Interfac. Mater.*, vol. 1 pp. 49–55, 2013.

[30] N. Chehata, A. Ltaief, R. Bkakri, A. Bouazizi, and E. Beyou, "Conducting polymer functionalized multi-walled carbon nanotubes nanocomposites: Optical properties and morphological characteristics," *Mater. Lett.*, vol. 121, pp. 227–230, 2014.

[31] R. A. Janssen, M. P. Christiaans, C. Hare, N. Martin, N. S. Sariciftci, A. J. Heeger, F. Wudl, "Photoinduced electron transfer reactions in mixed films of conjugated polymers and a homologous series of tetracyanopquinodimethane derivatives," *J. Chem. Phys.*, vol. 103, pp. 8840–88451995.

[32] Z. Sun, Z. Yan, J. Yao, E. Beitler, Y. Zhu, and J. M. Tour, "Growth of graphene from solid carbon sources," Nature, vol. 468, pp. 549–552, 2010.

[33] S. Sarkar, E. Bekyarova, and R.C. Haddon, "Chemistry at the dirac point: diels_alder reactivity of graphene," *Acc. Chem. Res.*, vol. 45, pp.673–682, 2012.

[34] [A. Moliton, and J. M. Nunzi, "How to model the behaviour of organic photovoltaic cells," Polym. Int., vol. 55, pp. 583–600, 2006.